

RESEARCH LETTER

10.1029/2017GL076666

Key Points:

- Climatologies overestimate oxygen concentrations and underestimate denitrification in the Gulf of Oman because of insufficient sampling
- Submesoscale and mesoscale processes regulate oxygen concentrations by stirring oxygenated Persian Gulf Water throughout the oxygen minimum zone
- Spiciness serves as a physical proxy for determining low oxygen concentrations in the Gulf of Oman

Supporting Information:

- Supporting Information S1
- Figure S1
- Movie S1

Correspondence to:

B. Y. Queste,
b.queste@uea.ac.uk

Citation:

Queste, B. Y., Vic, C., Heywood, K. J., & Piontkovski, S. A. (2018). Physical controls on oxygen distribution and denitrification potential in the north west Arabian Sea. *Geophysical Research Letters*, 45, 4143–4152. <https://doi.org/10.1029/2017GL076666>

Received 7 DEC 2017

Accepted 28 MAR 2018

Accepted article online 27 APR 2018

Published online 5 MAY 2018

Corrected 22 MAY 2018

This article was corrected on 22 MAY 2018. See the end of the full text for details.

©2018. The Authors.

This is an open access article under the terms of the Creative Commons Attribution License, which permits use, distribution and reproduction in any medium, provided the original work is properly cited.

Physical Controls on Oxygen Distribution and Denitrification Potential in the North West Arabian Sea

Bastien Y. Queste¹ , Clément Vic² , Karen J. Heywood¹ , and Sergey A. Piontkovski³ 

¹Centre for Ocean and Atmospheric Sciences, School of Environmental Sciences, University of East Anglia, Norwich, UK,

²Department of Ocean and Earth Sciences, University of Southampton, Southampton, UK, ³College of Agricultural and Marine Sciences, Sultan Qaboos University, Muscat, Oman

Abstract At suboxic oxygen concentrations, key biogeochemical cycles change and denitrification becomes the dominant remineralization pathway. Earth system models predict oxygen loss across most ocean basins in the next century; oxygen minimum zones near suboxia may become suboxic and therefore denitrifying. Using an ocean glider survey and historical data, we show oxygen loss in the Gulf of Oman (from 6–12 to <2 $\mu\text{mol kg}^{-1}$) not represented in climatologies. Because of the nonlinearity between denitrification and oxygen concentration, resolutions of current Earth system models are too coarse to accurately estimate denitrification. We develop a novel physical proxy for oxygen from the glider data and use a high-resolution physical model to show eddy stirring of oxygen across the Gulf of Oman. We use the model to investigate spatial and seasonal differences in the ratio of oxic and suboxic water across the Gulf of Oman and waters exported to the wider Arabian Sea.

Plain Language Summary Oxygen is present in the ocean and is required by all marine plants and animals to breathe. In certain regions around the world, oxygen concentrations reach very low levels. These are known as “oxygen minimum zones”. When oxygen is absent, chemical cycling of nitrogen, a key nutrient for plant growth, changes dramatically. Computer simulations of ocean oxygen show a decrease in oxygen over the next century and growing oxygen minimum zones. However, these simulations have a difficult time representing small but very important features such as eddies, which impact how oxygen is transported. It is difficult to predict what will happen in the biggest of the world’s oxygen minimum zones, the Arabian Sea, as piracy and geopolitical tensions have limited past opportunities for observing these processes. To remedy this, we deployed two remote-controlled submarines, known as a Seagliders, in the Gulf of Oman. These instruments measured a strong decrease of oxygen in the oxygen minimum zone compared to pre-1990 values. We then combined the Seaglider data with a very high resolution computer simulation to determine how oxygen is spread around the northwestern Arabian Sea throughout different seasons and the monsoons.

1. Introduction

Oxygen is necessary to sustain aerobic life; it regulates biogeochemical cycling and structures marine ecosystems. Oxygen minimum zones (OMZ; oxygen concentrations much lower than saturation) generally refer to specific regions with midwater concentrations below 60 $\mu\text{mol kg}^{-1}$ (hypoxic) such as the eastern tropical Pacific, the northern Indian Ocean and, to a lesser extent, the eastern tropical Atlantic (Stramma et al., 2010). Deoxygenation in the marine environment is a critical global issue and is now an investigative program of the United Nations Intergovernmental Oceanographic Commission (Altieri & Gedan, 2015; Löscher et al., 2016). Earth system models (ESMs) predict deoxygenation across many ocean basins, including the Arabian Sea (Bopp et al., 2013; Long et al., 2016; Stramma et al., 2010). Despite significant uncertainty under Coupled Model Intercomparison Project Phase 5 scenarios, this oxygen decline is a cause for concern as deoxygenation leads to expansion of OMZs. The importance of deoxygenation is particularly pronounced along the edges of OMZs where large volumes of water are near suboxic concentrations (6 $\mu\text{mol kg}^{-1}$), below which biogeochemical cycling pathways change significantly. OMZs are central to oceanic nitrogen cycling as denitrification and anaerobic ammonium oxidation occur only under suboxic (< 6 $\mu\text{mol kg}^{-1}$) and anoxic (< 0.1 $\mu\text{mol kg}^{-1}$) conditions, respectively (Bange et al., 2005).

The Arabian Sea is home to the thickest and most intense OMZ worldwide (Figure 1), with suboxic concentrations between 150 and 1,000 m (Bange et al., 2005; Banse et al., 2014; McCreary et al., 2013; Piontkovski

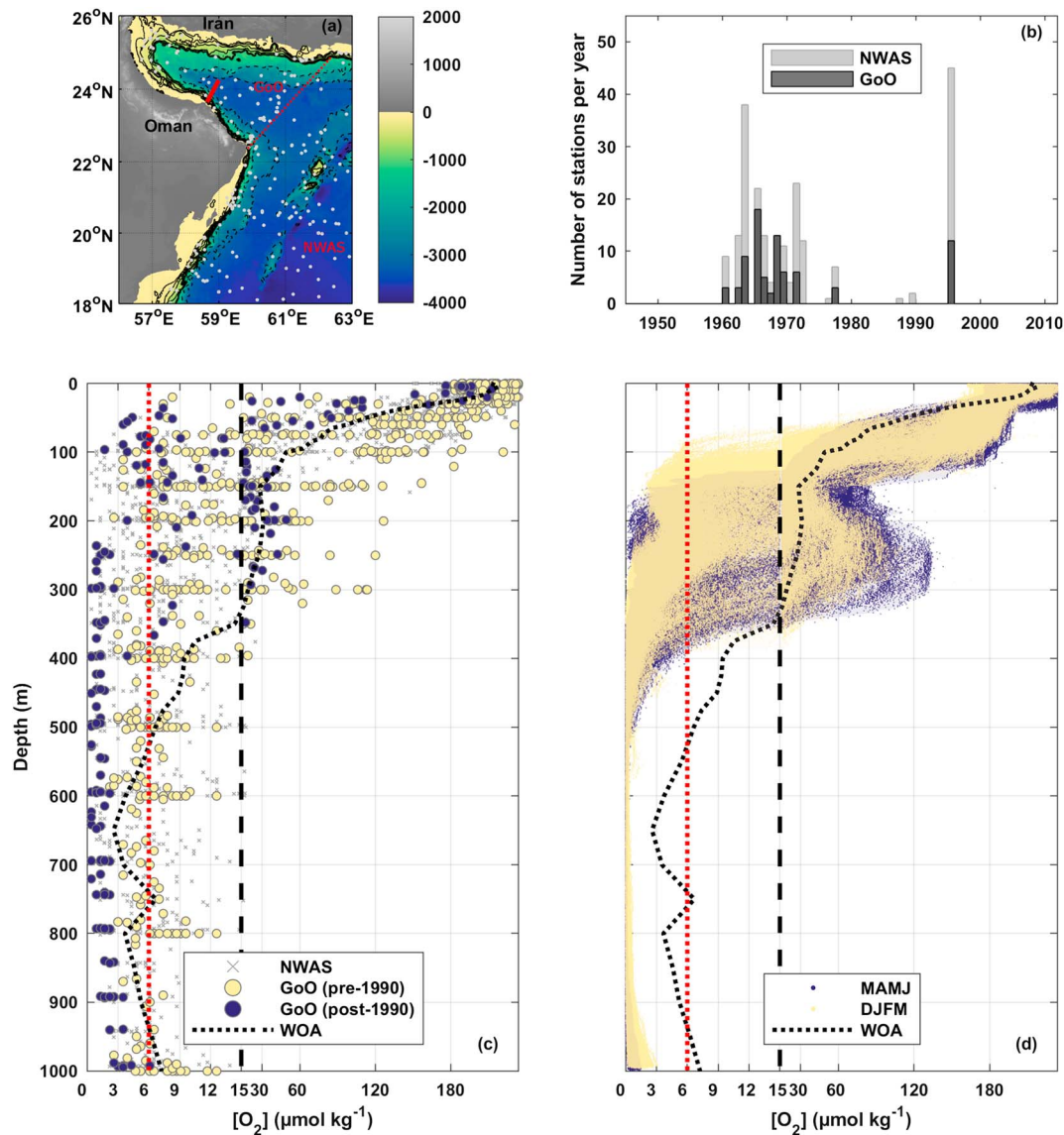


Figure 1. (a) Bathymetric map of the northwest Arabian Sea (NWAS) and location of the glider sections (thick red line). The Gulf of Oman (GoO) region described in this paper is delimited by the dotted red line at its eastern boundary, coincident with the seasonal Ras-Al-Hadd jet. All historical stations from Hydrobase 3 are indicated by gray dots. Historical oxygen data of the NWAS from Hydrobase 3 are presented (b) chronologically and as (c) vertical profiles. Glider oxygen profiles are shown in Figure 1d. Note the split abscissa at $15 \mu\text{mol kg}^{-1}$ for clarity at suboxic concentrations. Annual climatological profile of dissolved oxygen concentration from the World Ocean Atlas 2013 at the glider transect location is shown by the dotted black line, and the limit between suboxic and oxic waters ($6 \mu\text{mol kg}^{-1}$) is shown by the dotted red line in Figures 1c and 1d.

& Al-Oufi, 2015; Piontkovski & Queste, 2016). It is responsible for 50% of the global OMZ denitrification budget (Ward et al., 2009). Despite this crucial impact on the global ocean nitrogen budget, political and logistical difficulties as well as the prevalence of piracy have hampered observational programs in the region since the Joint Global Ocean Flux Study (JGOFS) in the 1990s (Figure 1b). Most of the western Indian Ocean is projected to undergo weak deoxygenation with moderate confidence over the next century under Coupled Model Intercomparison Project Phase 5 scenarios (Bopp et al., 2013; Long et al., 2016; Stramma et al., 2010). However the Gulf of Oman (Figure 1a) is projected to undergo stronger deoxygenation with much greater confidence (Bopp et al., 2013; Long et al., 2016; Stramma et al., 2010). Piontkovsky and Queste (2016) described ongoing deoxygenation trends in the northwestern Arabian Sea (NWAS) and a shoaling OMZ over the past three decades. Here we separate the Gulf of Oman and the NWAS at the Ras-Al-Hadd jet (Figure 1), a seasonal barotropic current that extends northeastward from Oman's easternmost point. We consider the Gulf of Oman and the NWAS to be hydrographically distinct

regions. The Gulf of Oman is generally warmer and does not show significant seasonal upwelling, whereas the NWAS is cooler due to the strong and persistent seasonal upwelling linked to the monsoon along the eastern coast of Oman (Böhm et al., 1999; Vic et al., 2017). The Ras-Al-Hadd jet limits exchanges between the Gulf of Oman and the NWAS, leading to prolonged residence times within the Gulf.

The fate of Persian Gulf Water (PGW) can be summarized as follows (L'Hégaret et al., 2016, 2015; Vic et al., 2015). At the western end of the Gulf of Oman, PGW exits the Persian Gulf through the shallow Strait of Hormuz. PGW is transported by a continental slope current driven by gravitational adjustment and is rapidly transformed through isopycnal mixing across the Gulf of Oman (Bower et al., 2000), spreading between 150 and 350 m, overlapping with the upper OMZ, on the western boundary of the Gulf of Oman and Arabian Sea. Remotely formed mesoscale eddies propagate westward into the Gulf of Oman and interact with the southern shelf slope, leading to PGW shedding by both mesoscale and submesoscale features. PGW is ultimately stirred and mixed in the interior of the Gulf of Oman and the northern Arabian Sea by two large persistent eddies at the western and eastern ends of the Gulf of Oman, respectively, and by numerous smaller eddies shed by the shelf slope currents (Vic et al., 2015). The animation provided as supporting information illustrates the interaction of these mesoscale and submesoscale eddies throughout 2 years of model output. Details of the model are included in the supporting information (Risien & Chelton, 2008; Shchepetkin & McWilliams, 2005; Vic et al., 2014; Worley et al., 2005). This water mass is then exported out to the NWAS and spreads both southward and eastward and can be traced across the Indian Ocean. Therefore, the extent of stirring and mixing within the Gulf of Oman and the NWAS impacts the oxygen content of water exported across the Indian Ocean (Jain et al., 2016; Lachkar et al., 2016).

Modeling work by Lachkar et al. (2016) shows that PGW eddies transport oxygen to the wider OMZ, reducing denitrification, increasing surface nitrogen supply, and suppressing OMZ expansion. They emphasize the need to better understand the processes as existing parameterizations of eddy-driven oxygen fluxes are insufficient to resolve the submesoscale variability observed in oxygen concentrations and its impacts on nitrogen budgets. Pelagic denitrification is a bacterial process whereby fixed nitrogen (most often as nitrate) is converted to dissolved dinitrogen gas (Bange et al., 2005); this occurs primarily under suboxic conditions as oxygen becomes less favorable as an electron donor. Suboxic OMZs account for 30–50% of oceanic nitrogen loss through denitrification and produce large amounts of the greenhouse gas nitrous oxide (Bange et al., 2005; Codispoti et al., 2001; Ji et al., 2015; Löscher et al., 2016). Note that although OMZ are sites of intense nitrous oxide production per surface area, global nitrous oxide production is still dominated by nitrification (> 90%; Freing et al., 2012). As a water mass transitions from hypoxic to suboxic conditions, denitrification suddenly becomes an important and dominant process (Löscher et al., 2016). In other words, a small shift in oxygen concentrations near the oxygen denitrification threshold will trigger a complete change in nitrogen cycling pathways. It is therefore critical to resolve oxygen concentrations at the submesoscale. As the relationship between oxygen concentrations and denitrification is nonlinear (i.e., occurs below $6 \mu\text{mol kg}^{-1}$ and is absent above), a misrepresentation of oxygen variability, such as occurring in coarse ESMs, causes strong errors in estimates of denitrification. The more heterogeneous the distribution of hypoxic and suboxic water is, the greater the potential for incorrectly assessing the volume of water that may be denitrifying.

Here we demonstrate using historical climatology and an ocean glider time series that the core of the OMZ in the Gulf of Oman has shifted from a hypoxic to a suboxic regime. We illustrate that this shift is not represented in widely used climatologies and may negatively impact accuracy of projections of deoxygenation in ESM. We use the glider observations to show the importance of mesoscale and submesoscale features in stirring oxygen across the Gulf. Finally, we extend the glider observations using a high-resolution physical model of the region to assess the seasonally varying extent of suboxia in the Gulf.

2. The Gulf of Oman: From Hypoxic to Suboxic

Observations in the region, and therefore climatologies (e.g., World Ocean Atlas 2013 (WOA13) data in Figures 1c and 1d), are skewed toward the 1960s (first International Indian Ocean Experiment; IIOE) and the 1990s (JGOFS): two intense periods of sampling followed by sharp declines in observational effort (Figure 1b). Oxygen measurements pre-JGOFS available in Hydrobase 3 (Curry, 1996) show an ecosystem on the verge of suboxia (Figure 1c); oxygen concentrations primarily lie within $6\text{--}12 \mu\text{mol kg}^{-1}$ throughout the OMZ with a few isolated profiles exhibiting concentrations between 3 and $6 \mu\text{mol kg}^{-1}$. Data from JGOFS

post-1990 systematically show concentrations below $3 \mu\text{mol kg}^{-1}$ throughout the OMZ. This suggests a decreasing trend in oxygen concentration, but the scarcity of data has hitherto prevented any definite statement.

During both glider campaigns, throughout 2015 and 2016, both gliders observed little temporal variability in oxygen concentrations in the surface layer (0 to 100 m) and below 450 m (Figure 1d). Between 100 and 450 m, the gliders showed high temporal and horizontal variability in conservative temperature (13.5 to 23.2°C), absolute salinity (36.13 to 38.23 g kg^{-1}), and oxygen (< 2 to $140 \mu\text{mol kg}^{-1}$); this corresponds to the intermittent PGW outflow visible along the $26.2 \sigma_\theta$ isopycnal in Figure 2. Below 450 m, the OMZ was persistently suboxic, with concentrations below $2 \mu\text{mol kg}^{-1}$ in the core of the OMZ (450–1,000 m; Figure 1d). The oxygen optodes deployed on the gliders do not have the resolution or accuracy at extremely low oxygen concentrations to confidently state that the gliders sampled anoxic waters; limitations in the calibration method also impose a $\pm 1 \mu\text{mol kg}^{-1}$ error on glider oxygen values. Despite these limitations, the glider observations clearly demonstrate concentrations at or below $1 \pm 1 \mu\text{mol kg}^{-1}$ throughout the core of the OMZ. Details of glider data processing are included in the supporting information (Benson & Krause Jr., 1984; Dee et al., 2011; Frajka-Williams et al., 2011; Garau et al., 2011; Queste, 2014).

Within the top 150 m, oxygen data from both glider deployments, historical records, and WOA13 agree, showing a decrease in oxygen with depth from $>180 \mu\text{mol kg}^{-1}$ near the surface to hypoxic concentrations at 150 m. At depths greater than 150 m, WOA13 best represents the data collected pre-1990 (Figure 1d) while nearly all data points from 1990 onward are lower oxygen concentrations than the climatology (with the exception of a band between 150 and 300 m where PGW is located). The glider data match the distribution of the historical data collected post-1990 with suboxic concentrations below 350 m and highly variable oxygen concentrations (< 2 to $140 \mu\text{mol kg}^{-1}$) between 150 and 350 m.

There are insufficient observations to determine whether deoxygenation occurred within the PGW layer (150–350 m). A previous study suggested that the oxycline had shoaled based on historical data (Piontkovski & Queste, 2016); however, this is not apparent in the glider data. Rather, the glider data suggest a seasonal pattern in oxycline depth, which may have been incorrectly identified as a longer trend previously through seasonal biases in sampling. Noticeably, the oxygen measurements obtained from the glider confirm the deoxygenation trend suggested by the JGOFS data from post-1990 (Figure 1). The combination of later historical data (post-1990), recent regional studies (Piontkovski & Queste, 2016), and the 2015–2016 glider observations clearly demonstrates a strong decline in oxygen content of the Gulf of Oman and water exported to the NWS, currently unreported in the literature. The historical data (Figure 1c) and glider observations (Figure 1d) show a shift from severe hypoxia to persistently suboxic conditions between IIOE and JGOFS.

As a result of the intense sampling effort during IIOE and the low number of stations during and after JGOFS, observations after IIOE are insufficiently weighted to provide an accurate estimate of present conditions (Figures 1c and 1d). WOA13 under-represents the volume of suboxic water observed by later historical data and the glider observations. Because ESMs (Bopp et al., 2013; Long et al., 2016; Stramma et al., 2010) and regional models of the NWS (Lachkar et al., 2016) are restored to biased climatologies (Piontkovski & Queste, 2016), estimates of future oxygen concentrations are likely to be erroneous.

3. Eddy Stirring of Oxygen

Figure 2 shows two glider sections (section 2, 16–21 March 2015; and section 14, 27–30 April 2015) and a composite of all sections collected by SG579 (March–June 2015). PGW is present between 150 and 350 m with its core along the $26.2 \sigma_\theta$ isopycnal, where the upper boundary of the OMZ would otherwise be located, and is characterized by an elevated oxygen signature extending offshore from the shelf slope (Figure 2). Previous studies relying on in situ data, satellite altimetry, and regional models have highlighted the importance of eddies in transporting PGW in the Gulf of Oman (L'Hégaret et al., 2016, 2015; Vic et al., 2015). Large annually recurrent anticyclonic flows driven by monsoonal wind stress (L'Hégaret et al., 2016, 2015) and smaller cyclonic and anticyclonic submesoscale eddies are generated by interactions between the mesoscale propagating eddies and local topography (Vic et al., 2015). The animation (supporting information) illustrates the scale and variability of both the mesoscale and submesoscale eddies and confirms the identification of these features in the glider observations and model. Glider sections

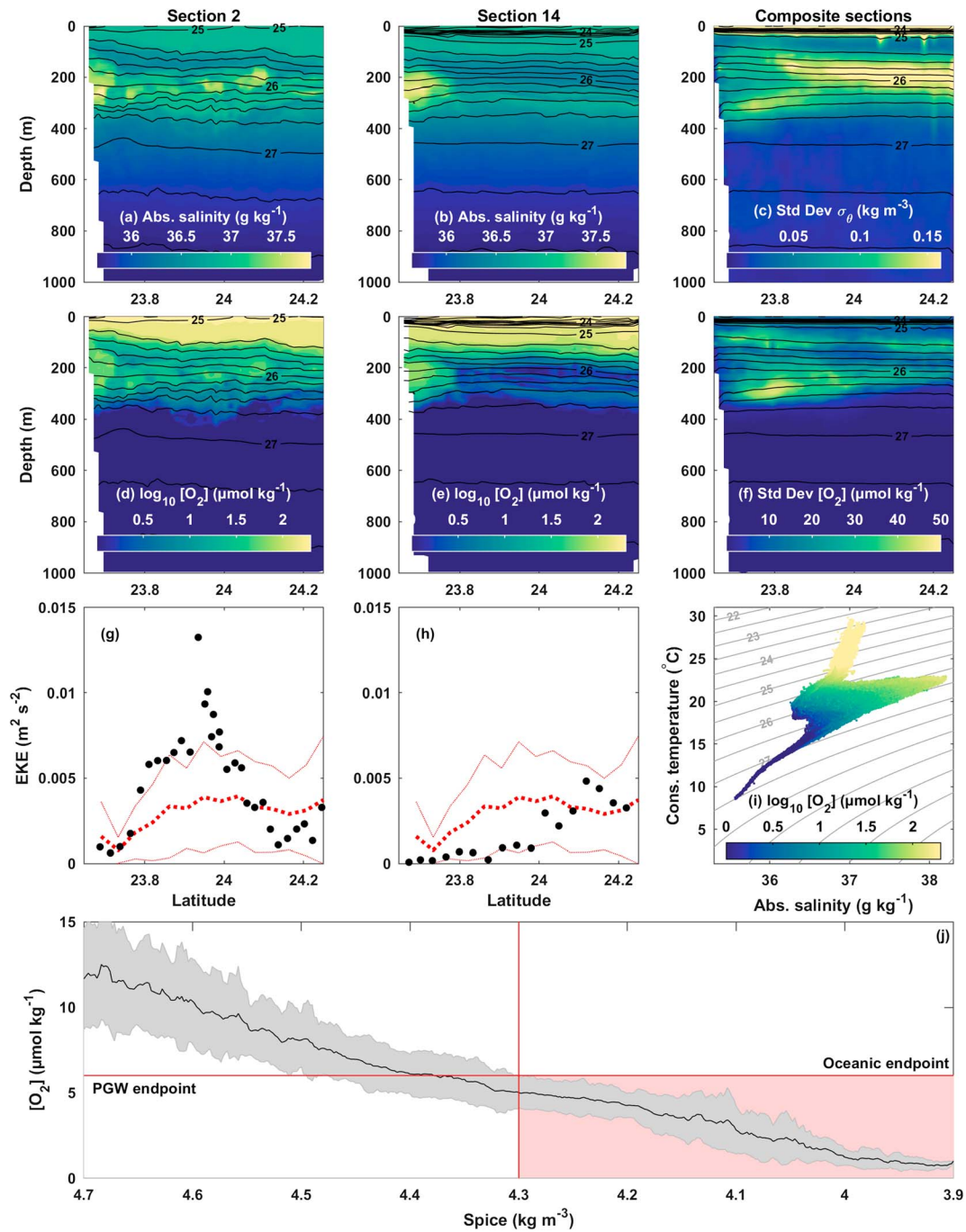


Figure 2. Two example sections of (a and b) absolute salinity (g kg^{-1}) and (d and e) dissolved oxygen (displayed on a log scale, $\mu\text{mol kg}^{-1}$), overlaid by isopycnals (kg m^{-3}), from SG579 representing periods of both high (Figures 2a, 2d, and 2g) and low (Figures 2b, 2e, and 2h) eddy kinetic energy (EKE; g and h; $\text{m}^2 \text{s}^{-2}$). EKE is shown as a black dot for each dive within the section, while the red lines show mean plus and minus the standard deviation of EKE across all of SG579's transects. (c, f, and i) Standard deviation across all transects for absolute salinity (Figure 2c; g kg^{-1}) and dissolved oxygen (Figure 2f; $\mu\text{mol kg}^{-1}$), overlaid by mean isopycnals (kg m^{-3}) across all sections. Figure 2i is a temperature-salinity plot (Figure 2i; $^{\circ}\text{C}$ and g kg^{-1}). Figure 2j shows the mean relation (and standard deviation in gray) of dissolved oxygen concentrations to spice along the $26 \pm 0.1 \sigma_{\theta}$ isopycnal. The red lines separate hypoxic and suboxic conditions at the 4.3 kg m^{-3} spice contour. Note the inverse abscissa in Figure 2c. Persian Gulf Water is denoted as PGW.

(Figures 2a–2f) show sloping isopycnals along the entire transect (76 km) resulting from the mesoscale persistent eddies within the Gulf (visible in Figures 3a–3d and supporting information). This is accompanied by an increase in mean eddy kinetic energy (EKE) away from the shelf edge (Figures 2g and 2h). EKE for each glider dive was calculated as half of the squared difference between per-dive detided dive-averaged

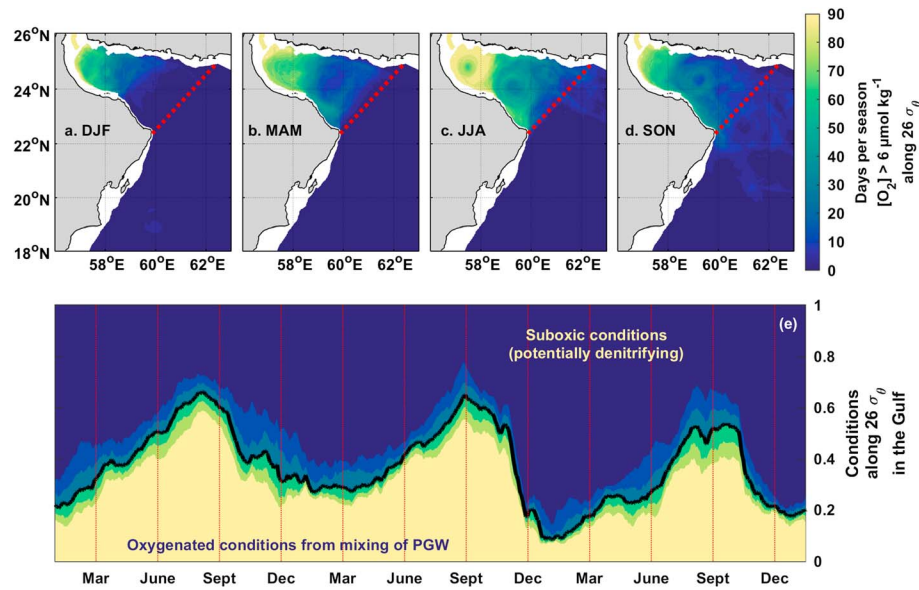


Figure 3. Estimated distribution in both (a–d) space and (e) time of suboxic water using spiciness below 4.3 kg m^{-3} as a proxy within the Persian Gulf Water (PGW) layer. Figures 3a–3d show the proportion of the 90-day season where oxygenated water is present from PGW ($> 6 \mu\text{mol kg}^{-1}$). Figure 3e shows the extent of suboxic water across the Sea of Oman throughout the three model years, as delimited by the red line in Figures 3a–3d. The black line indicates the 4.3 kg m^{-3} spiciness threshold, with colored contours showing the sensitivity of the spiciness threshold at 0.1 kg m^{-3} intervals. Seasons are indicated as DJF (December–February), MAM (March–May), JJA (June–August), and SON (September–November).

currents and the local spatial and temporal mean detided dive-averaged currents obtained over each glider campaign.

While both sections show similar influence from mesoscale eddies, sections 2 and 14 illustrate two contrasting EKE regimes at the submesoscale. The elevated EKE was associated with submesoscale heterogeneity in salinity and oxygen along the density surfaces where the PGW is present (Figures 2a, 2d, and 2g). Throughout both deployments, elevated EKE was also associated with vertical intrusions of hypoxic water; in section 2, this is visible as an oxygenated patch intruding below the $26.8 \sigma_{\theta}$ isopycnals, between 23.9°N and 24°N (Figure 2a). The data available do not allow us to identify whether these intrusions are related to horizontal transport or vertical motions associated with eddies. Figure 2d shows the scale of oxygen variability with suboxic and hypoxic concentrations alternating at scales of less than 10 km along the $26.2 \sigma_{\theta}$ isopycnal. These submesoscale features (horizontal heterogeneity and vertical intrusions) are most likely associated with rapidly moving submesoscale eddies generated near the shelf edge (Vic et al., 2015). In contrast, during periods of low EKE, a strong homogeneous core of PGW flows eastward along the shelf edge and salinity and oxygen are reduced in the offshore region (Figure 2b).

The composite glider sections (Figures 2c and 2f) illustrate how the combination of stirring from both mesoscale and submesoscale eddies leads to offshore transport of high salinity hypoxic water through the suboxic OMZ. The glider observations confirm that the salinity and oxygen properties of water exported to the NWAS are temporally variable and dependent on eddy dynamics within the Gulf of Oman.

4. Seasonality and Implications of Eddy Stirring

Next, we illustrate the seasonal variability in suboxic volume within the Gulf of Oman. The complexity of biogeochemical models is such that performing high-resolution fully coupled biogeochemical runs is generally too computationally expensive to be done over large spatial or temporal scales. To this end, we identify a novel physical proxy for oxygen concentrations, which we use to extend a regional circulation model resolving the relevant submesoscale features identified in the previous section. Understanding the seasonal variability of suboxic volume in turn provides insight into the seasonal variability of denitrification potential within the Gulf of Oman and NWAS region.

Because of its warmer and more saline nature relative to Indian Ocean Equatorial Water at the same density, PGW is easily traced through spiciness. Spiciness is a variable measuring water mass characteristics on

isopycnals, where warmer, more saline water masses are spicier (McDougall & Krzysik, 2015). In contrast, we refer to colder, fresher water masses as mintier. Elevated oxygen concentrations observed in this layer are directly associated with the PGW (Figure 2) and can thus be directly related to a local maximum in spice. Overall, there is a strong correlation between spice and oxygen concentration below the surface layer, whereby spicy water masses show greater oxygen concentrations while the minty Indian Ocean Equatorial Water (spice values below 4 kg m^{-3}) is near anoxia. Due to slow remineralization rates at depth (particularly low oxygen water) and the absence of production below the photic zone, transport and mixing are the dominant processes defining oxygen gradients at the interface between the PGW and the suboxic OMZ. Spiciness was found to be a better indicator of oxygen concentration than salinity, temperature, or density alone. Figure 2j shows how the spice contour of 4.3 kg m^{-3} effectively separates hypoxic and suboxic water masses. We investigate this particular oxygen threshold as it separates denitrifying from nondenitrifying water masses, and the small scale variability in these water masses will determine the pelagic nitrogen cycle. The glider observations show that in the Gulf of Oman and Arabian Sea, where high salinity and oxygenated water masses are present and transported across the basin-wide OMZ (Jain et al., 2016; Lachkar et al., 2016), spiciness is a novel and useful proxy for oxygen at low concentrations and can be used to distinguish between hypoxic and suboxic water masses in physical models.

Using the glider-derived oxygen to spice relationship (Figure 2j), spice from the model is used to estimate the spread of dissolved oxygen across the Gulf of Oman and NWAS (Figures 2 and 3). The hydrostatic model does not resolve the range of mixing processes occurring at the Strait of Hormuz (Thoppil et al., 2009; Vic et al., 2015), and the resulting PGW is slightly shallower (core at 200 m) and lighter ($26 \sigma_\theta$) than in the observations (250 m and $26.2 \sigma_\theta$; supporting information). To best represent the PGW core, the analysis of the model output is performed on the $26 \sigma_\theta$ isopycnal. Due to biases in the model and the nature of this proxy, the results cannot be used to quantify an absolute suboxic volume for the Gulf of Oman. The model does however resolve the relevant physical processes, identified in the glider observations, and provides a robust estimate of seasonal variability. The results were not sensitive to the choice of spiciness contour (Figure 3e). Different spice thresholds show the same relative seasonal variability of suboxic extent along the $26 \sigma_\theta$ isopycnal. Seasonality of the outflow properties (temperature, salinity, and rate of flow) of PGW is primarily driven by the annual cycle in evaporation in the Persian Gulf that yields variations in sinking rate and properties of newly formed PGW (Johns et al., 2003; Swift & Bower, 2003). Within the Regional Ocean Modeling System (ROMS) configuration, these properties are prescribed and consistent between years, and the atmospheric forcing is driven by monthly climatologies. Interannual differences in the extent of suboxia in Figure 3 are therefore due to internal model variability and by exchanges at the Arabian Sea boundary with the parent solution. Seasonal differences in suboxic volume are driven by both atmospheric forcing and seasonal differences of outflow properties.

The model shows substantial seasonal variability in distribution of oxygen, with the fraction of oxic water ($> 6 \mu\text{mol kg}^{-1}$) across the Gulf varying from 0.15 (January Year 3) to 0.65 (August Year 1) along the $26 \sigma_\theta$ isopycnal (Figure 3e). Seasonal differences in oxygenated PGW extent along the $26 \sigma_\theta$ isopycnal are particularly large, with PGW creating persistent oxic conditions across the western half of the Gulf of Oman between 150 and 350 m and showing high variability in the eastern half at the peak of summer (Figures 3a–3d). In the winter, PGW water is constrained to the southern margin and is only occasionally transported across the Gulf of Oman as eddies entrain oxygenated water from the PGW outflow along the slope. As a result, there is a 2 to 4 times increase of the extent of more oxygenated water ($> 6 \mu\text{mol kg}^{-1}$) along the $26 \sigma_\theta$ isopycnal surface from winter to summer. Figure 3 shows interannual variability in winter oxic extent (0.35 in Year 1 to 0.1 in Year 3); interannual variability during the summer monsoon is reduced but still present as shown by the increase in suboxic conditions in September in the third year. The model accurately resolves the two persistent eddies in the Gulf of Oman (Figures 3a–3d; animation in the supporting information) that exhibit intermittent elevated oxygen concentrations ($> 6 \mu\text{mol kg}^{-1}$), highlighting their importance as sites of oxygen distribution within the Gulf and therefore regulators of oxygen content export out to the NWAS (Figure 3). As the PGW spreads below the thermocline, at the same depth as the OMZ's upper boundary, the presence (or absence) of PGW plays a key role in regulating the depth of the oxycline. As the intensity of denitrification has been linked to remineralization depth (Al Azhar et al., 2017), a deeper suboxic boundary not only reduces suboxic volume of the OMZ but may inhibit denitrification within the depth range where denitrification would otherwise be stronger.

Such variability in oxycline depth will impact fisheries. The region is home to several high-biomass species that have been shown to tolerate oxygen concentrations as low as $20 \mu\text{mol kg}^{-1}$ (*Euphausia diomedea*, Seibel et al., 2016; Myctophids, Torres et al., 2012). Many pelagic organisms in the NWS have shown specific adaptations and exceptional tolerance to low-oxygen conditions (Torres et al., 2012). Stramma et al. (2010, 2012) have demonstrated strong feedbacks between shoaling hypoxia and habitat compression for higher-trophic level species. In conditions such as those observed in the Gulf of Oman and the NWS, PGW forms refugia of intermediate oxygen concentrations ($20 < [\text{O}_2] < 140 \mu\text{mol kg}^{-1}$) where predation is greatly reduced; these hypoxic conditions are habitable to specially adapted, smaller and less metabolically active prey species while larger predators are limited to the surface oxygenated layer (Bianchi et al., 2013; Sperling et al., 2013). In addition, stable oxygen concentrations lead to low species diversity while the marginal regions show elevated diversity (Gooday et al., 2009). Such patterns have been confirmed along the Omani and Pakistani margins (Gooday et al., 2009; Levin et al., 2000) and are likely strongly affected by the PGW outflow. Therefore, the seasonality in oxygen stirring and OMZ volume that we observe will have significant impacts on species diversity and fisheries catch and recruitment.

5. Conclusions

This study has shown that the midwater decline in oxygen content of the NWS after IIOE has led to persistent suboxic conditions in the OMZ (150 m–950 m) in the absence of PGW. Currently reported conditions in the literature and represented in climatologies do not reflect this decline, overestimating oxygen concentrations and likely underestimating denitrification. The unique hydrographic properties of the region lead to high variability in OMZ volume with a strong seasonal pattern driven by the stirring of PGW by eddies. Interannual variability in stirring will have a significant impact on the contributions of the NWS to the wider Arabian Sea OMZ.

The Gulf of Oman is a site of persistent suboxia that is traditionally not quantified in denitrification estimates because of outdated climatologies. The extent of the OMZ fluctuates on mesoscale eddy temporal and spatial scales, requiring high-resolution modeling to accurately represent mesoscale and submesoscale stirring in this highly dynamic region. This area needs further investigation if we are to properly parameterize eddy-driven oxygen fluxes in the ESMs used to predict future ecosystems. Management of the fisheries and ecosystems of the western Indian Ocean over coming decades will depend crucially on better understanding and forecasting of the oxygen budget of the Gulf of Oman. This in turn depends upon the future export and eddy stirring of PGW that may alter under climate change.

Acknowledgments

This work was supported by the ONR GLOBAL grants N62909-14-1-N224/SQU, Sultan Qaboos University grants EG/AGR/FISH/14/01 and IG/AGR/FISH/17/01, and UK NERC grants NE/M005801/1 and NE/N012658/1. We thank Benjamin G. M. Webber for his insightful comments during the writing of this manuscript, and we thank Burton Jones and the other reviewers for taking the time to review the manuscript. We are grateful to the UEA Seaglider Facility and Sultan Qaboos University technical staff for their technical help with instruments and deployments. We also extend our thanks to the Five Oceans Environmental Services consultancy, who saved a struggling glider at the drop of a hat. The glider data are available on request from the UEA Seaglider Facility and from the British Oceanographic Data Centre (doi:10.5285/697eb954-f60c-603b-e053-6c86abc00062).

References

- Al Azhar, M., Lachkar, Z., Lévy, M., & Smith, S. (2017). Oxygen minimum zone contrasts between the Arabian Sea and the Bay of Bengal implied by differences in remineralization depth. *Geophysical Research Letters*, *44*, 11,106–11,114. <https://doi.org/10.1002/2017GL075157>
- Altieri, A. H., & Gedan, K. B. (2015). Climate change and dead zones. *Global Change Biology*, *21*(4), 1395–1406. <https://doi.org/10.1111/gcb.12754>
- Bange, H. W., Naqvi, S. W. A., & Codispoti, L. a. (2005). The nitrogen cycle in the Arabian Sea. *Progress in Oceanography*, *65*(2-4), 145–158. <https://doi.org/10.1016/j.pocean.2005.03.002>
- Banase, K., Naqvi, S. W. A., Narvekar, P. V., Postel, J. R., & Jayakumar, D. A. (2014). Oxygen minimum zone of the open Arabian Sea: Variability of oxygen and nitrite from daily to decadal timescales. *Biogeosciences*, *11*(8), 2237–2261. <https://doi.org/10.5194/bg-11-2237-2014>
- Benson, B. B., & Krause, D. Jr. (1984). The concentration and isotopic fractionation of oxygen dissolved in freshwater and seawater in equilibrium with the atmosphere. *Limnology and Oceanography*, *29*(3), 620–632. <https://doi.org/10.4319/lo.1984.29.3.0620>
- Bianchi, D., Galbraith, E. D., Carozza, D. A., Mislán, K. A. S., & Stock, C. A. (2013). Intensification of open-ocean oxygen depletion by vertically migrating animals. *Nature Geoscience*, *6*(7), 545–548. <https://doi.org/10.1038/ngeo1837>
- Böhm, E., Morrison, J. M., Manghnani, V., Kim, H.-S., & Flagg, C. N. (1999). The Ras al Hadd jet: Remotely sensed and acoustic Doppler current profiler observations in 1994–1995. *Deep Sea Research Part II: Topical Studies in Oceanography*, *46*(8–9), 1531–1549. [https://doi.org/10.1016/S0967-0645\(99\)00034-X](https://doi.org/10.1016/S0967-0645(99)00034-X)
- Bopp, L., Resplandy, L., Orr, J. C., Doney, S. C., Dunne, J. P., Gehlen, M., et al. (2013). Multiple stressors of ocean ecosystems in the 21st century: Projections with CMIP5 models. *Biogeosciences*, *10*(10), 6225–6245. <https://doi.org/10.5194/bg-10-6225-2013>
- Bower, A. S., Hunt, H. D., & Price, J. F. (2000). Character and dynamics of the Red Sea and Persian Gulf outflows. *Journal of Geophysical Research*, *105*(C3), 6387–6414. <https://doi.org/10.1029/1999JC900297>
- Codispoti, L. A., Brandes, J. A., Christensen, J. P., Devol, A. H., Naqvi, S. W. A., Paerl, H. W., & Yoshinari, T. (2001). The oceanic fixed nitrogen and nitrous oxide budgets: Moving targets as we enter the anthropocene? *Scientia Marina*, *65*(S2), 85–105. <https://doi.org/10.3989/scimar.2001.65s285>
- Curry, R. G. (1996). *HYDROBASE: A database of hydrographic stations and tools for climatological analysis*. Woods Hole, MA: Woods Hole Oceanographic Institution. <https://doi.org/10.1575/1912/472>
- Dee, D. P., Uppala, S. M., Simmons, A. J., Berrisford, P., Poli, P., Kobayashi, S., et al. (2011). The ERA-Interim reanalysis: Configuration and performance of the data assimilation system. *Quarterly Journal of the Royal Meteorological Society*, *137*(656), 553–597. <https://doi.org/10.1002/qj.828>

- Frajka-Williams, E., Eriksen, C. C., Rhines, P. B., & Harcourt, R. R. (2011). Determining vertical water velocities from Seaglider. *Journal of Atmospheric and Oceanic Technology*, 28(12), 1641–1656. <https://doi.org/10.1175/2011JTECH0830.1>
- Freing, A., Wallace, D. W. R., & Bange, H. W. (2012). Global oceanic production of nitrous oxide. *Philosophical Transactions of the Royal Society, B: Biological Sciences*, 367(1593), 1245–1255. <https://doi.org/10.1098/rstb.2011.0360>
- Garau, B., Ruiz, S., Zhang, W. G., Pascual, A., Heslop, E., Kerfoot, J., & Tintoré, J. (2011). Thermal lag correction on Slocum CTD glider data. *Journal of Atmospheric and Oceanic Technology*, 28(9), 1065–1071. <https://doi.org/10.1175/JTECH-D-10-05030.1>
- Gooday, A. J., Levin, L. A., Aranda da Silva, A., Bett, B. J., Cowie, G. L., Dissard, D., et al. (2009). Faunal responses to oxygen gradients on the Pakistan margin: A comparison of foraminiferans, macrofauna and megafauna. *Deep-Sea Research Part II: Topical Studies in Oceanography*, 56(6–7), 488–502. <https://doi.org/10.1016/j.dsr2.2008.10.003>
- Jain, V., Shankar, D., Vinayachandran, P. N., Kankonkar, A., Chatterjee, A., Amol, P., et al. (2016). Evidence for the existence of Persian Gulf water and Red Sea water in the Bay of Bengal. *Climate Dynamics*, 48(9–10), 3207–3226. <https://doi.org/10.1007/s00382-016-3259-4>
- Ji, Q., Babbitt, A. R., Jayakumar, A., Oleynik, S., & Ward, B. B. (2015). Nitrous oxide production by nitrification and denitrification in the eastern tropical South Pacific oxygen minimum zone. *Geophysical Research Letters*, 42, 10,755–10,764. <https://doi.org/10.1002/2015GL066853>
- Johns, W. E., Yao, F., Olson, D. B., Josey, S. A., Grist, J. P., & Smeed, D. A. (2003). Observations of seasonal exchange through the Straits of Hormuz and the inferred heat and freshwater budgets of the Persian Gulf. *Journal of Geophysical Research*, 108(C12), 3391. <https://doi.org/10.1029/2003JC001881>
- Lachkar, Z., Smith, S., Lévy, M., & Pauluis, O. (2016). Eddies reduce denitrification and compress habitats in the Arabian Sea. *Geophysical Research Letters*, 43, 9148–9156. <https://doi.org/10.1002/2016GL069876>
- Levin, L. A., Gage, J. D., Martin, C., & Lamont, P. A. (2000). Macrobenthic community structure within and beneath the oxygen minimum zone, NW Arabian Sea. *Deep Sea Research Part II: Topical Studies in Oceanography*, 47(1–2), 189–226. [https://doi.org/10.1016/S0967-0645\(99\)00103-4](https://doi.org/10.1016/S0967-0645(99)00103-4)
- L'Hégaret, P., Carton, X., Louazel, S., & Boutin, G. (2016). Mesoscale eddies and submesoscale structures of Persian Gulf water off the Omani coast in spring 2011. *Ocean Science*, 12(3), 687–701. <https://doi.org/10.5194/os-12-687-2016>
- L'Hégaret, P., Duarte, R., Carton, X., Vic, C., Ciani, D., Baraille, R., & Corréard, S. (2015). Mesoscale variability in the Arabian Sea from HYCOM model results and observations: Impact on the Persian Gulf water path. *Ocean Science*, 11(5), 667–693. <https://doi.org/10.5194/os-11-667-2015>
- Long, M. C., Deutsch, C., & Ito, T. (2016). Finding forced trends in oceanic oxygen. *Global Biogeochemical Cycles*, 30, 381–397. <https://doi.org/10.1002/2015GB005310>
- Löscher, C. R., Bange, H. W., Schmitz, R. A., Callbeck, C. M., Engel, A., Hauss, H., et al. (2016). Water column biogeochemistry of oxygen minimum zones in the eastern tropical North Atlantic and eastern tropical South Pacific oceans. *Biogeosciences*, 13(12), 3585–3606. <https://doi.org/10.5194/bg-13-3585-2016>
- McCreary, J. P., Yu, Z., Hood, R. R., Vinayachandran, P. N., Furue, R., Ishida, A., & Richards, K. J. (2013). Dynamics of the Indian-Ocean oxygen minimum zones. *Progress in Oceanography*, 112–113, 15–37. <https://doi.org/10.1016/j.pocean.2013.03.002>
- McDougall, T. J., & Krzysik, O. A. (2015). Spiciness. *Journal of Marine Research*, 73(5), 141–152. <https://doi.org/10.1357/002224015816665589>
- Piontkovski, S. A., & Al-Oufi, H. S. (2015). The Omani shelf hypoxia and the warming Arabian Sea. *International Journal of Environmental Studies*, 72(2), 256–264. <https://doi.org/10.1080/00207233.2015.1012361>
- Piontkovski, S. A., & Queste, B. Y. (2016). Decadal changes of the western Arabian Sea ecosystem. *International Aquatic Research*, 8(1), 49–64. <https://doi.org/10.1007/s40071-016-0124-3>
- Queste, B. Y. (2014). *Hydrographic observations of oxygen and related physical variables in the North Sea and western Ross Sea Polynya*. Norwich, UK: University of East Anglia.
- Risien, C. M., & Chelton, D. B. (2008). A global climatology of surface wind and wind stress fields from eight years of QuikSCAT scatterometer data. *Journal of Physical Oceanography*, 38(11), 2379–2413. <https://doi.org/10.1175/2008JPO3881.1>
- Seibel, B. A., Schneider, J. L., Kaartvedt, S., Wishner, K. F., & Daly, K. L. (2016). Hypoxia tolerance and metabolic suppression in oxygen minimum zone Euphausiids: Implications for ocean deoxygenation and biogeochemical cycles. *Integrative and Comparative Biology*, 56(4), 510–523. <https://doi.org/10.1093/icb/icw091>
- Shchepetkin, A. F., & McWilliams, J. C. (2005). The regional oceanic modeling system (ROMS): A split-explicit, free-surface, topography-following-coordinate oceanic model. *Ocean Modelling*, 9(4), 347–404. <https://doi.org/10.1016/j.ocemod.2004.08.002>
- Sperling, E. A., Frieder, C. A., Raman, A. V., Girguis, P. R., Levin, L. A., & Knoll, A. H. (2013). Oxygen, ecology, and the Cambrian radiation of animals. *Proceedings of the National Academy of Sciences of the United States of America*, 110(33), 13446–13451. <https://doi.org/10.1073/pnas.1312778110>
- Stramma, L., Prince, E. D., Schmidtko, S., Luo, J., Hoolihan, J. P., Visbeck, M., et al. (2012). Expansion of oxygen minimum zones may reduce available habitat for tropical pelagic fishes. *Nature Climate Change*, 2(1), 33–37. <https://doi.org/10.1038/nclimate1304>
- Stramma, L., Schmidtko, S., Levin, L. A., & Johnson, G. C. (2010). Ocean oxygen minima expansions and their biological impacts. *Deep Sea Research Part I: Oceanographic Research Papers*, 57(4), 587–595. <https://doi.org/10.1016/j.dsr.2010.01.005>
- Swift, S. A., & Bower, A. S. (2003). Formation and circulation of dense water in the Persian/Arabian Gulf. *Journal of Geophysical Research*, 108(C1), 3004. <https://doi.org/10.1029/2002JC001360>
- Thoppil, P. G., Hogan, P. J., Thoppil, P. G., & Hogan, P. J. (2009). On the mechanisms of episodic salinity outflow events in the Strait of Hormuz. *Journal of Physical Oceanography*, 39(6), 1340–1360. <https://doi.org/10.1175/2008JPO3941.1>
- Torres, J. J., Grigsby, M. D., & Clarke, M. E. (2012). Aerobic and anaerobic metabolism in oxygen minimum layer fishes: The role of alcohol dehydrogenase. *Journal of Experimental Biology*, 215(11), 1905–1914. <https://doi.org/10.1242/jeb.060236>
- Vic, C., Capet, X., Roulet, G., & Carton, X. (2017). Western boundary upwelling dynamics off Oman. *Ocean Dynamics*, 67(5), 585–595. <https://doi.org/10.1007/s10236-017-1044-5>
- Vic, C., Roulet, G., Capet, X., Carton, X., Molemaker, M. J., & Gula, J. (2015). Eddy-topography interactions and the fate of the Persian Gulf outflow. *Journal of Geophysical Research: Oceans*, 120, 6700–6717. <https://doi.org/10.1002/2015JC011033>
- Vic, C., Roulet, G., Carton, X., & Capet, X. (2014). Mesoscale dynamics in the Arabian Sea and a focus on the Great Whirl life cycle: A numerical investigation using ROMS. *Journal of Geophysical Research: Oceans*, 119, 6422–6443. <https://doi.org/10.1002/2014JC009857>
- Ward, B. B., Devol, A. H., Rich, J. J., Chang, B. X., Bulow, S. E., Naik, H., et al. (2009). Denitrification as the dominant nitrogen loss process in the Arabian Sea. *Nature*, 461(7260), 78–81. <https://doi.org/10.1038/nature08276>
- Worley, S. J., Woodruff, S. D., Reynolds, R. W., Lubker, S. J., & Lott, N. (2005). ICOADS release 2.1 data and products. *International Journal of Climatology*, 25(7), 823–842. <https://doi.org/10.1002/joc.1166>

Erratum

In the originally published version of this article, several instances of the notation of units were incorrectly typeset. Throughout the article, $\mu\text{mol kg}^{-1}$ had been wrongly changed to $\mu\text{mol/kg}^{-1}$, and kg m^{-3} had been changed to kg/m^3 . These errors have since been corrected, and the present version may be considered the authoritative version of record.